Received April 19, 2019, accepted May 14, 2019, date of publication May 22, 2019, date of current version June 10, 2019.

Digital Object Identifier 10.1109/ACCESS.2019.2918299

Optimal Configuration Analysis of AOA Localization and Optimal Heading Angles Generation Method for UAV Swarms

WEIJIA WANG[1], PENG BAI[1], YU ZHOU[2], XIAOLONG LIANG[1], AND YUBING WANG[1]

[1]Air Traffic Control and Navigation College, Air Force Engineering University, Xi'an 710051, China
[2]Equipment Management & UAV Engineering College, Air Force Engineering University, Xi'an 710051, China

Corresponding author: Yu Zhou (15398033290@163.com)

This work was supported in part by the National Science Foundation of China under Grant 61502523 and Grant 61703427, in part by the Natural Science Foundation Research Project of Shanxi Province under Grant 2017JQ6035, and in part by the Shanxi Province Laboratory of Metasynthesis for Electronic and Information System.

ABSTRACT In this paper, the angle-of-arrival (AOA) measurements are adapted to locate a target using the UAV swarms equipped with passive receivers. The measurement noise is considered to be target-to-receiver distance dependent. The Cramer–Rao low bound (CRLB) of the AOA localization is calculated, and the optimal deployments are explored through changing angular separations and distances. Then, a distributed collaborative autonomous generation (DCAG) method is proposed based on the deep neural network (NN). The off-line training and on-line application rules are applied to generate the optimal heading angles for the UAV swarms in the AOA localization. The simulation results show that through the DCAG method, the generated heading angles for UAV swarms enhance the localization accuracy and stability.

INDEX TERMS AOA localization, distributed collaborative autonomous generation (DCAG), Cramer-Rao low bound (CRLB), deep neural network (NN).

I. INTRODUCTION

Localization of a radio frequency (RF) with static and movable sensor platforms has received significant interest in both civil and defense applications, such as search, rescue, and surveillance. The purpose of passive localization is to estimate the location of a target by processing the emitter signals, which is widely applied in wireless sensor networks (WSN) [1]–[4]. Currently, localization in sensor networks using passive measurements can be based on various type of measurements such as time difference of arrival (TDOA) [1], angle of arrival (AOA) [2] as well as received signal strength (RSS) [3], etc. AOA localization, which is predicated on the triangulation of AOA lines emanating from multiple receivers, has been a research area of significant interest for several decades.

The AOA measurements can be calculated by maximum likelihood (ML) estimator [4], pseudo-linear estimator [5], etc. The Recursive algorithm based on extended Kalman filter (EKF) was also applied for tracking moving targets using bearings-only measurements [6], [7]. It is well known that the performance of localization is highly related to the receiver-target deployment [1]–[10]. Therefore, an optimal deployment can further improve the localization accuracy. The optimal receiver-target deployment analyzed by the Fisher information matrix (FIM) had been explored in [8]–[10]. Paper [8] provided the rigorous proof of the relative receiver-target deployment for AOA localization. Paper [9] mainly studied the optimal angular receiver separation. In [10], the optimal receiver-target geometries for both TDOA and AOA localization were identified and studied. In paper [11], AOA localization in three-dimensional space was applied based on the Cramer-Rao low bound (CRLB). Most of the works deal with AOA optimal deployment with independent and changeless variance. In this paper, we firstly studied a more realistic model, where the localization error variance is target-to-receiver distance dependent. The optimal deployments of AOA localization are explored through angle and distance criteria based on the CRLB.

Recently, passive localization with UAV swarms has great potential in military reconnaissance, anti-terrorism stability and emergency response [12]. Therefore, we extend our work to the application of AOA localization with UAV swarms. How to generate real-time heading angles of UAV swarms

The associate editor coordinating the review of this manuscript and approving it for publication was Long Cheng.

on-line and realize the optimal dynamic receiver-target deployments have become one of the hot research issues. For this issue, the centralized real-time optimization (CRTO) method [13] was applied and FIM was adopted as the optimization function for path planning optimization. Then, the combined heading angles of UAV swarms that corresponding to the maximum value of the determinant of the FIM are calculated within each time step. There are two weaknesses in this method. One is that the passive localization accuracy is sensitive to the heading angles of UAV swarms. With the increase of the number of UAVs, the space of the optional combined heading angles increases exponentially, which leads to large calculation delay and is difficult to meet the needs of high maneuvering target localization. The other is that structure of CRTO is centralized, which increases the communication delay and results poor stability.

Aiming at the problems of CRTO method, this paper proposes a Distributed Cooperative and Autonomous Generation (DCAG) method, which is based on neural network (NN) [14]. Neural network (NN) methods have been broadly applied to optimal control [15], [16], collision avoidance [17], coverage [18], but most of them deal with single UAV or robot [19] and cannot be applied in the cooperative localization mission. This method contains two parts. The first part is the off-line training, large-sample simulations of UAV swarms and target data set in different deployments are generated based on the analysis of CRLB. The optimal heading angles data set are constructed to explore whether a deep neural network can effectively be used to learn optimal heading angles of UAV swarms from different deployments. The second part is on-line application, the autonomous and rapid output of optimal heading angles are generated through to ensure the improvement of localization. Therefore, the problem of generating real-time optimization of heading angles with large amount of computation is transformed into a distributed online prediction problem with low power consumption and time delay, which makes the problem effectively solved.

The remainder of this paper is organized as follows. Problem description and modeling are given in Sec. II and performance analysis of AOA localization based on CRLB is given in Section III. In Sec. VI, The CRTO method is given. Then, DCAG method is proposed in Sec. V. These algorithms are verified via simulation results of UAV swarms, in Sec. VI, and finally Sec. VII concludes the paper.

II. PROBLEM DESCRIPTION AND MODELING

We consider the situation with M receivers localizing a target in the 2D. The state vector of each movable receiver is $\chi_i(k) = \left[\mathbf{x}_i(k)^T, \dot{\mathbf{x}}_i(k)^T\right]^1, i = 1, 2, \cdots M$, where $\mathbf{x}_i(k) = [x_i(k), y_i(k)]^T$ is the position and $\dot{\mathbf{x}}_i(k) = [\dot{x}_i(k), \dot{y}_i(k)]^T$ represents the velocity vector. Let $\mathbf{x}_t = [x_t, y_t]^T \in \mathbb{R}^2$ be the unknown location of an emitter, r_i is the distance between emitter and the$i$-th receiver, i.e. $r_i = \|\mathrm{x}_t - \mathrm{x}_i\|$. Then AOA estimate equation by the receiver can be written as [8]

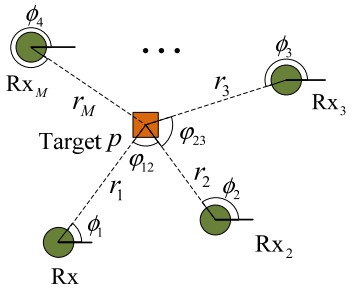

FIGURE 1. AOA localization geometry with M receivers.

$$\hat{\phi}_i = \phi_i(\mathbf{x}_t) + e_i \tag{1}$$

where $\phi_i(\mathrm{x}_t) = \arctan 2(x_t - x_i, y_t - y_i)$ .e_i is the measurement error and is assumed to be zero-mean Gaussian white noise with variance σ_i^2, i.e. $e_i \sim \mathcal{N}(0, \sigma_i^2)$.

For assumption of distance-dependent noise, the variance of localization error is inversely proportional to the SNR of the signal, and the SNR is inversely proportional to the distance between the target and the i-th receiver r_i^2. Therefore, the i-th receiver error can be written as [20]:

$$\sigma_i^2(r) = \begin{cases} \dfrac{a}{SNR_0} \cdot \dfrac{r_i^2}{r_0^2} & r_i > r_0 \\ \dfrac{a}{SNR_0} & r_i \le r_0 \end{cases} \tag{2}$$

where, r_0 is the lower bound distance that corresponding to the minimum of localization error variance, SNR_0 is the minimum value of SNR and a is a constant path-loss exponent.

Fig. 1 shows AOA localization geometry with M receivers. The measurement vector from M receivers can be written as $\widehat{\mathbf{\Phi}}(\mathbf{x}_t) = \mathbf{\Phi}(\mathbf{x}_t) + \mathbf{e}$, where $\mathbf{\Phi}(\mathbf{x}_t) = [\phi_1(\mathbf{x}_t), \cdots, \phi_N(\mathbf{x}_t)]^T$, $\mathbf{e} = [e_1, \cdots, e_N]^T$, with the covariance $\mathbf{R}_r = diag\left[\sigma_1^2, \sigma_2^2, \cdots, \sigma_M^2\right]$.

The purpose of this paper is to improve the performance of AOA localization using UAV swarms, we firstly focus on the performance analysis of optimal AOA receiver-target deployments. These explicit solutions can provide the tactical guidance for the UAV swarms placement problem.

III. PERFORMANCE ANALYSIS BASED ON CRLB

As for an unbiased estimate $\hat{\mathbf{x}}$ of $\mathbf{x}$, the CRLB can be expressed as:

$$E\left[(\mathbf{x} - \hat{\mathbf{x}})(\mathbf{x} - \hat{\mathbf{x}})^T\right] \ge \mathbf{J}^{-1} \triangleq \mathbf{CRLB}(\mathbf{x}) \tag{3}$$

where, $\mathbf{J}$ is the corresponding FIM.

For the measurement vector $\widehat{\mathbf{\Phi}} = \mathbf{\Phi}(\mathbf{x}) + \mathbf{e}$, the FIM is given by

$$\mathbf{J}_{i,j} = E\left[\frac{\partial}{\partial x_i}\ln(f_{\widehat{\mathbf{\Phi}}}(\widehat{\mathbf{\Phi}}; \mathbf{x}))\frac{\partial}{\partial x_j}\ln(f_{\widehat{\mathbf{\Phi}}}(\widehat{\mathbf{\Phi}}; \mathbf{x}))\right] \tag{4}$$

where the $f_{\widehat{\Phi}}(\widehat{\mathbf{\Phi}};\mathbf{x})$ is the probability density function (PDF) of the AOA measurement vector $\widehat{\mathbf{\Phi}}$

$$f_{\widehat{\Phi}}(\widehat{\mathbf{\Phi}};\mathbf{x})=\frac{1}{(2\pi)^{M/2}|\mathbf{R}|^{1/2}} \exp\left[-\frac{1}{2}(\widehat{\mathbf{\Phi}}-\mathbf{\Phi}(\mathbf{x}))^T\mathbf{R}^{-1}(\widehat{\mathbf{\Phi}}-\mathbf{\Phi}(\mathbf{x}))\right] \quad (5)$$

Inspired by paper [20], the FIM for AOA localization with distance-dependent noise is given by

$$\mathbf{J}_{(i,j)}=\underbrace{\frac{1}{\sigma^2(\mathbf{x}_t)}\frac{\partial\mathbf{\Phi}(\mathbf{x}_t)}{\partial x_i}\frac{\partial\mathbf{\Phi}(\mathbf{x}_t)}{\partial x_j}}_{\mathbf{J}_{1,(i,j)}}+\underbrace{\frac{1}{2}\frac{1}{\sigma^2(\mathbf{x}_t)}\frac{\partial\sigma(\mathbf{x}_t)}{\partial x_i}\frac{\partial\sigma(\mathbf{x}_t)}{\partial x_j}}_{\mathbf{J}_{2,(i,j)}} \quad (6)$$

Therefore, this FIM consists of two terms. The first term, $\mathbf{J}_1$ denotes the FIM of the measurement estimation and can be rewritten as

$$\mathbf{J}_{1,(i,j)}=\nabla_P\mathbf{\Phi}(\mathbf{x}_t)^T\mathbf{R}_r^{-1}\nabla_P\mathbf{\Phi}(\mathbf{x}_t) \quad (7)$$

with

$$\begin{cases}\mathbf{J}_{1,(1,1)}=\sum_{i=1}^{M}\frac{\sin^2\phi_i}{\beta r_i^4}\\ \mathbf{J}_{1,(1,2)}=\mathbf{J}_{1,(2,1)}=-\sum_{i=1}^{M}\frac{\sin\phi_i\cos\phi_i}{\beta r_i^4}\\ \mathbf{J}_{1,(2,2)}=\sum_{i=1}^{M}\frac{\cos^2\phi_i}{\beta r_i^4}\end{cases} \quad (8)$$

where $\beta=\frac{a}{SNR_0 r_0^2}$. As for the second term, when $r_i > r_0$, $\mathbf{J}_2$ is the FIM of localization error variance, which can be expanded as

$$\mathbf{J}_{2,(i,j)}=\frac{1}{2}Tr\left(\mathbf{R}_r^{-1}(\mathbf{x})\frac{\partial\mathbf{R}_r(\mathbf{x})}{\partial x_i}\mathbf{R}_r^{-1}(\mathbf{x})\frac{\partial\mathbf{R}_r(\mathbf{x})}{\partial x_j}\right) \quad (9)$$

where,

$$\begin{cases}\frac{\partial\mathbf{R}_r(x)}{\partial x_1}=2\beta diag\left[r_1\cos\phi_1, r_2\cos\phi_2,\cdots,r_M\cos\phi_M\right]\\ \frac{\partial\mathbf{R}_r(x)}{\partial x_2}=2\beta diag\left[r_1\sin\phi_1, r_2\sin\phi_2,\cdots,r_M\sin\phi_M\right]\end{cases} \quad (10)$$

Thus, the entire FIM with distance-dependent noise of AOA localization can be shown as (11), as shown at the top of the next page.

Denote that $c_i=2/r_i^2+1/\beta r_i^4$ and $d_i=2/r_i^2-1/\beta r_i^4$, $\mathbf{J}$ can be simplified as (12), as shown at the top of the next page.

Therefore, the determinant of FIM and the CRLB can be expressed as

$$\det(\mathbf{J})=4\sum_{i=1}^{M}\sum_{j=i+1}^{M}d_i d_j\sin^2(\phi_j-\phi_i)+\left(\sum_{i=1}^{M}c_i\right)^2-\left(\sum_{i=1}^{M}d_i\right)^2 \quad (13)$$

$$\mathbf{CRLB}=\mathbf{J}^{-1}=\frac{1}{\det(\mathbf{J})}\begin{bmatrix}\mathbf{J}_{22} & -\mathbf{J}_{12}\\ -\mathbf{J}_{21} & \mathbf{J}_{11}\end{bmatrix} \quad (14)$$

According to the A-optimality [21], the trace of the CRLB is applied as the objective function to evaluate performance of AOA localization:

$$tr(\mathbf{J}^{-1})=\frac{\sum_{i=1}^{M}c_i}{\det(\mathbf{J})}=\frac{4\sum_{i=1}^{M}c_i}{\left(\sum_{i=1}^{M}c_i\right)^2-\left(\sum_{i=1}^{M}d_i\cos 2\phi_i\right)^2-\left(\sum_{i=1}^{M}d_i\sin 2\phi_i\right)^2} \quad (15)$$

According to the A-optimality, the optimal deployment can be acquired, when the minimum value of trace of CRLB is obtained. From (15), it obvious that $tr\left(\mathbf{J}^{-1}\right)$ is a function of $\mathbf{\Phi}$ and $\mathbf{r}$. Hence, the optimal deployments are explored through changing angular separations $\mathbf{\Phi}$ and distances $\mathbf{r}$ changing cases.

A. ANGLE CHANGING CASE

When $r_i, i \in \{1,\cdots,M\}$ are given arbitrarily but fixed, from (15), the maximization of $\det(\mathbf{J})$ is equivalent to the minimization of $tr(\mathbf{J}^{-1})$. For convenience, the optimization objective function is

$$\arg\max_{\phi_1,\cdots,\phi_M} f(\Phi)=4\sum_{i=1}^{M}\sum_{j=i+1}^{M}d_i d_j\sin^2(\phi_j-\phi_i)+\left(\sum_{i=1}^{M}c_i\right)^2-\left(\sum_{i=1}^{M}d_i\right)^2 \quad (16)$$

When $M=2$, (16) is solved when $\phi_2-\phi_1=k\frac{\pi}{2}$, $(k=1,3)$. Let $\varphi_{ij}=[0,\pi)$ be the subtended angle between the i-th and j-th receivers. Thus we can obtain that $\varphi_{12}=\frac{\pi}{2}$, which means orthogonal receiver-target geometry is the optimal deployment in this situation.

When $M=3$, (16) takes the form

$$f(\mathbf{\Phi}=4\left(d_1d_2\sin^2\varphi_{12}+d_1d_3\sin^2\varphi_{13}+d_2d_3\sin^2(\varphi_{13}-\varphi_{12})\right)+\left(\sum_{i=1}^{3}c_i\right)^2-\left(\sum_{i=1}^{3}d_i\right)^2 \quad (17)$$

By taking the partial derivative of (17) with respect to the variables φ_{12} and φ_{13} respectively, we can get

$$\begin{cases}d_1d_2\sin(2\varphi_{12})-d_2d_3\sin(2\varphi_{13}-2\varphi_{12})=0\\ d_1d_3\sin(2\varphi_{13})+d_2d_3\sin(2\varphi_{13}-2\varphi_{12})=0\end{cases} \quad (18)$$

Then by solving the above two equations, the optimal angular separation φ_{12}, φ_{13} can be solved [8]

$$\begin{cases}\varphi_{12}=\left|\frac{1}{2}\arccos(\frac{d_3^2-d_2^2-d_1^2}{2d_1d_2})\right|\\ \varphi_{13}=\left|\frac{1}{2}\arccos(\frac{d_2^2-d_1^2-d_3^2}{2d_1d_3})\right|\end{cases} \quad (19)$$

$$\mathbf{J}=\begin{bmatrix} \sum_{i=1}^{M}\frac{\sin^2(\phi_i)}{\beta r_i^4}+2\sum_{i=1}^{M}\frac{\cos^2\phi_i}{r_i^2} & -\sum_{i=1}^{M}\frac{\sin(\phi_i)\cos(\phi_i)}{\beta r_i^4}+2\sum_{i=1}^{M}\frac{\cos\phi_i\sin\phi_i}{r_i^2} \\ -\sum_{i=1}^{M}\frac{\sin(\phi_i)\cos(\phi_i)}{\beta r_i^4}+2\sum_{i=1}^{M}\frac{\cos\phi_i\sin\phi_i}{r_i^2} & \sum_{i=1}^{M}\frac{\cos^2(\phi_i)}{\beta r_i^4}+2\sum_{i=1}^{M}\frac{\sin^2\phi_i}{r_i^2} \end{bmatrix} \tag{11}$$

$$\mathbf{J}=\begin{bmatrix} \frac{1}{2}\left(\sum_{i=1}^{M}c_i+\sum_{i=1}^{M}d_i\cos 2\phi_i\right) & \frac{1}{2}\sum_{i=1}^{M}d_i\sin 2\phi_i \\ \frac{1}{2}\sum_{i=1}^{M}d_i\sin 2\phi_i & \frac{1}{2}\left(\sum_{i=1}^{M}c_i-\sum_{i=1}^{M}d_i\cos 2\phi_i\right) \end{bmatrix} \tag{12}$$

Consider that the value of arccos(·) should be real, the real value holds when $d_m^2 \le \sum_{i=1,i\neq m}^{3} d_i^2, m \in \{1,\cdots,3\}$.

As for $d_m^2 > \sum_{i=1,i\neq m}^{3} d_i^2$, the maximizing value of $f(\mathbf{\Phi})$ is acquired when

$$\varphi_{km}=\frac{\pi}{2}, k=\{1,2,3\}\setminus m \tag{20}$$

where $\setminus$ is the set subtraction. The maximum value can be acquired by placing the m-th receiver in the vertical direction to the other receivers.

As for an arbitrary number $M \ge 4$ and arbitrary but fixed ranges, the following solutions can be acquired.

Corollary 1: When $M \ge 4$, let r_i be arbitrary but fixed for all $i \in \{1,\cdots,M>4\}$, then we have

$$f(\mathbf{\Phi}) \le \frac{1}{4}\left(\sum_{i=1}^{M}c_i\right)^2 \tag{21}$$

The equality holds if and only if

$$\left(\sum_{i=1}^{M}d_i\cos 2\phi_i\right)^2=0, \left(\sum_{i=1}^{M}d_i\sin 2\phi_i\right)^2=0 \tag{22}$$

Proof: By taking the derivative of (16) with respect to ϕ_s, $\forall s \in \{1,\cdots,M\}$, we can obtain

$$\begin{aligned} &\frac{\partial}{\partial\phi_s}\left(\sum_{i=1}^{M}\sum_{j=i+1}^{M}d_id_j\sin^2\left(\phi_j-\phi_i\right)\right) \\ &=\sum_{\substack{i=1\\ i\neq s}}^{M}d_sd_i\sin\left(2\left(\phi_s-\phi_i\right)\right) \\ &=d_s\sin(2\phi_s)\sum_{i=1}^{M}d_i\cos(2\phi_i)-d_s\cos(2\phi_s)\sum_{i=1}^{M}d_i\sin(2\phi_i) \\ &=\begin{bmatrix} d_s\sin(2\phi_s) & -d_s\cos(2\phi_s) \end{bmatrix}\begin{bmatrix} \sum_{i=1}^{M}d_i\cos(2\phi_i) \\ \sum_{i=1}^{M}d_i\sin(2\phi_i) \end{bmatrix} \\ &=0(s=1,\cdots,M) \end{aligned} \tag{23}$$

Therefore, all the M equations hold if and only if

$$\begin{cases} \sum_{i=1}^{M}d_i\cos(2\phi_i) \\ \sum_{i=1}^{M}d_i\sin(2\phi_i) \end{cases} \tag{24}$$

In this situation, the optimality configuration is heavily relies on frame theory [22], [23]. Then, the tight frame is solved for all $i \in \{1,\cdots,M\}$ if and only if

$$d_m^2 \le \sum_{i=1,i\neq m}^{M} d_i^2, m \in \{1,\cdots,M\} \tag{25}$$

In this situation, $f(\mathbf{\Phi})$ is upper-bounded by

$$\begin{aligned} f(\mathbf{\Phi})=\frac{1}{4}\left(\left(\sum_{i=1}^{M}c_i\right)^2-\left(\sum_{i=1}^{M}d_i\cos 2\phi_i\right)^2\right. \\ \left.-\left(\sum_{i=1}^{M}d_i\sin 2\phi_i\right)^2\right) \le \frac{1}{4}\left(\sum_{i=1}^{M}c_i\right)^2 \end{aligned} \tag{26}$$

Based on the tight frame, the optimal deployment is acquired when the frame is tight [24].

If $d_m^2 > \sum_{i=1,i\neq m}^{M} d_i^2, m \in \{1,\cdots,M\}, m \in \{1,\cdots,M\}$, no tight frames can be found. However, the tightest (but not tight) frame can be obtained. According to lemmas in [24], [25], the optimal deployment is acquire, if and only if

$$\varphi_{km}=\frac{\pi}{2}, k=\{1,\cdots,M\}\setminus m \tag{27}$$

Insert them into (16), $f(\mathbf{\Phi})$ is upper-bounded by

$$\frac{1}{4}\left(\left(\sum_{i=1}^{M} c_i\right)^2 - \left(d_m - \sum_{i=1, i\neq m}^{M} d_i\right)^2\right).$$

Here, we also consider the special case where all the receivers are placed on a circle centered at the target, i.e., the distances from the receivers to the target are all equal. In this situation, $r_1 = r_2 = \cdots = r_M = r$, where r is radius of the circle. Then the FIM can be written as:

$$\mathbf{J} = \begin{bmatrix} \frac{1}{2}\left(Mc_0 + d_0 \sum_{i=1}^{M} \cos 2\phi_i\right) & \frac{1}{2} d_0 \sum_{i=1}^{M} \sin 2\phi_i \\ \frac{1}{2} d_0 \sum_{i=1}^{M} \sin 2\phi_i & \frac{1}{2}\left(Mc_0 - d_0 \sum_{i=1}^{M} \cos 2\phi_i\right) \end{bmatrix} \tag{28}$$

where $c_0 = 2/r + 1/\beta r^4$, $d_0 = 2/r^2 - 1/\beta r^4$. From (28), we can derive the following optimization problem

$$\arg\max_{\phi_1,\cdots,\phi_M} f(\Phi) = \frac{1}{4}\left((Mc_0)^2 - d_0^2\left(\sum_{i=1}^{M} \cos 2\phi_i\right)^2 - d_0^2\left(\sum_{i=1}^{M} \sin 2\phi_i\right)^2\right) \tag{29}$$

When $M = 2$, It is obvious that the optimal configuration is $\varphi_{12} = \frac{\pi}{2}$.

Corollary 2: For equal receiver ranges $r_1 = r_2 = \cdots r_N = r$, $(N \geq 3)$, $f(\mathbf{\Phi})$ is bounded by

$$f(\mathbf{\Phi}) \leq \frac{1}{4}(Mc_0)^2 \tag{30}$$

the equality holds if and only if

$$\sum_{i=1}^{M} \cos(2\phi_i) = 0, \sum_{i=1}^{M} \sin(2\phi_i) = 0 \tag{31}$$

Then two special optimal configurations of the M receivers can be shown as below, which is the same as in paper [8]:

(1) Uniform angular arrays (UAAs):

$$\varphi_{ij} = \varphi_{ji} = \frac{2\pi}{M}, \quad \forall i, j \in \{1, \cdots, M\},\ j - i = 1 \tag{32}$$

(2) Non-uniform angular arrays (Non-UAAs):

$$\varphi_{ij} = \varphi_{ji} = \frac{\pi}{M}, \quad \forall i, j \in \{1, \cdots, M\},\ j - i = 1 \tag{33}$$

Proof: The proof consists of two parts. The first part is to find a lower bound for $f(\mathbf{\Phi})$, which is similar to *Corollary* 1, and the second part is to analyze the optimal configuration.

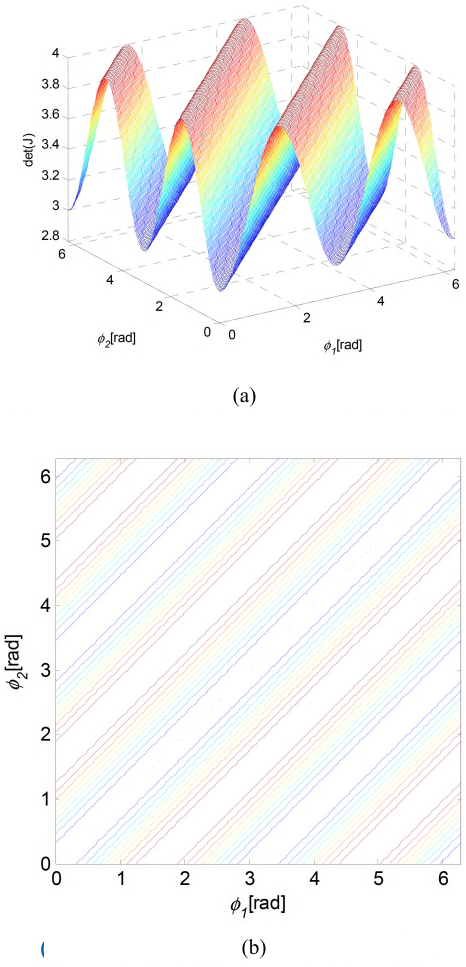

FIGURE 2. The variation of the determinant of FIM with equal receive ranges for $M = 2$. (a) The value of det (J) as a function of ϕ_1 and ϕ_2. (b) The contour plot of the value of det (J).

From (29), it is obvious that $f(\mathbf{\Phi})$ is upper bounded by

$$f(\mathbf{\Phi}) = \frac{1}{4}\left((Mc_0)^2 - d_0^2\left(\sum_{i=1}^{M} \cos 2\phi_i\right)^2 - d_0^2\left(\sum_{i=1}^{M} \sin 2\phi_i\right)^2\right) \leq \frac{1}{4}(Mc_0)^2 \tag{34}$$

where, $f(\mathbf{\Phi})$ is maximized if and only if (31) is simultaneously satisfied.

Example: Without loss of generality, let $c_0 = 2$, $d_0 = 1$. $f(\mathbf{\Phi})$ are calculated and the results are shown in Figs. 2 and 3, when $M = 2, 3$, respectively. When $M = 2$, the maximum value of $f(\Phi)$ is 4, which is obtained when $\phi_1 - \phi_2 = \frac{\pi}{2}$.

Figs. 3 shows the value of det $(\mathbf{J})$ and contour plot as a function of ϕ_2, ϕ_3 for $M = 3$. The maximum value of $f(\mathbf{\Phi})$ is 9, which is attained if $\{\theta_2, \theta_3\} \in \{\{60°, 120°\}, \{60°, 300°\}, \{120°, 60°\}, \{120°, 240°\}, \{240°, 120°\}, \{240°, 300°\}, \{300°, 60°\}, \{300°, 240°\}\}$.

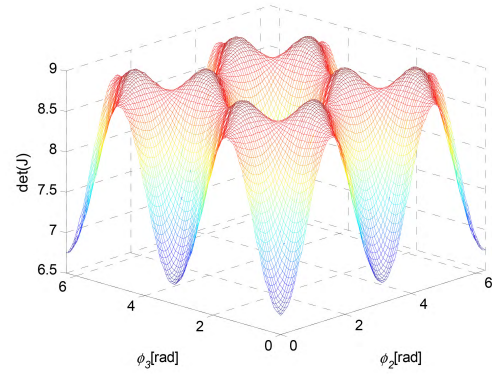

(a)

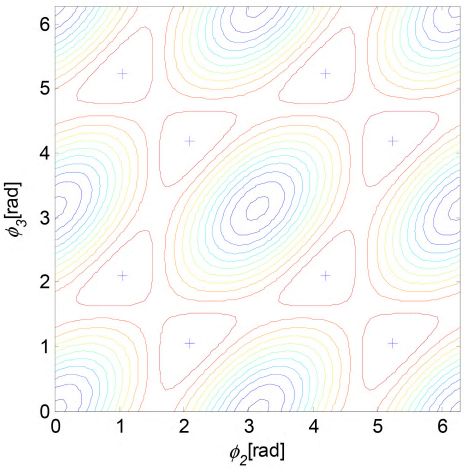

(b)

FIGURE 3. The variation of the determinant of FIM with equal receive ranges for $M = 3$. (a) The value of det (J) as a function of ϕ_2 and ϕ_3. (b) The contour plot of det (J) with maxima indicated with '+'.

In the angle changing case, the optimal angular receiver separation is not unique, there exist the optimal configuration with non-UAA angular receiver separation and also effected by the distance between receiver and target. The optimal angular separation provides the angle criterion for the optimal configuration.

B. DISTANCES CHANGING CASE

Consider the AOA localization problem, let the angle Φ be arbitrary but fixed, then the objective function can be written as

$$\arg\min_{r_1,\cdots,r_M} f(\mathbf{r}) = \frac{4\sum_{i=1}^{M} c_i}{\left(\sum_{i=1}^{M} c_i\right)^2 - \left(\sum_{i=1}^{M} d_i \cos 2\phi_i\right)^2 - \left(\sum_{i=1}^{M} d_i \sin 2\phi_i\right)^2} \tag{35}$$

where, $\phi_i, \forall i \in \{1, \cdots, M\}$ is arbitrary but fixed.

Corollary 3: When the angles $\mathbf{\Phi}$ is arbitrary but fixed, the shorter the distance r_i is, the less the value of $f(\mathbf{r})$ is. The minimum value of $f(\mathbf{r})$ is acquired when $r_i = r_{\min}$ $(i = 1, 2, \cdots, M)$.

Proof: From the meaning of $\mathbf{J}^{-1}$ and the fact that the measurement noise is larger when the distance r_i increases, $\mathbf{J}^{-1}$ shall increase. A similar proof can be found in [26] but is omitted here.

To sum up, the method of deployment optimization is to get close to the target, according to the distance criterion and select a good angular separation. The analysis of the optimal deployment helps to lay a foundation for waypoints optimization of UAV swarms and helps to understand optimization performance.

IV. TRADITIONAL CENTRALIZED REAL-TIME OPTIMIZATION (CRTO) METHOD

Sec. III gives the analysis of the optimal deployment without considering the constraints of the sensor platform, but in practical application, UAV receiving platforms are affected by their own motion constraints and cannot achieve the optimal deployment of the target location in a short time [27]. Especially in the absence of prior target information, UAV swarms need to transform the search configuration of the whole reconnaissance area into the location configuration of the key area and the key target. At initial time, the distance between the target and UAV swarms may be large, and it will take a certain time to achieve the optimal location and tracking configuration because of the influence of platform speed and turning angular rate. Therefore, how to improve the localization and tracking accuracy of the target through waypoint optimization is the problem to be solved.

Under the certain condition of signal processing and localization algorithm, it is necessary to optimize the real-time heading angles of UAV swarms by on-line combination, so as to directly determine waypoints in the next time step. From the analysis of CRLB, different values of CRLB can reflect the different deployments of UAV swarms. When the minimum value of CRLB is found, that means the optimal heading combination for the highest positioning accuracy.

Consider the target is located by M sensors, the ranges of UAV heading angles are between $[\Phi_{\min}, \Phi_{\max}]$. Denote ϑ as the number of alternative heading angles for UAV swarms at each moment, the decision-making spaces can be expressed as:

$$\Omega = \left(\frac{(\varphi_1 - \varphi_2)}{\vartheta}\right)^M \tag{36}$$

According to the above analysis, the optimal heading angles model is established with the optimal heading of each UAV at the next moment. The decision variable and the minimum CRLB is the objective function, which is a NP-Hard problem.

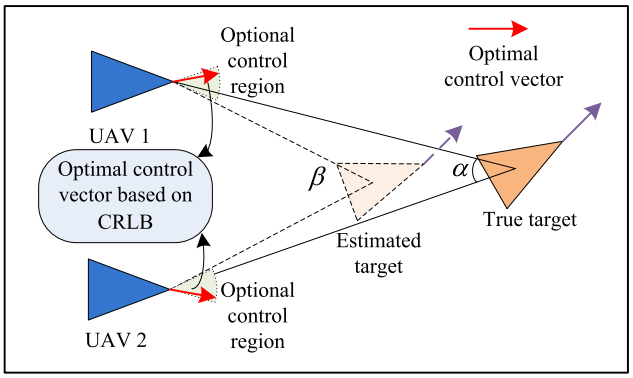

FIGURE 4. Illustration of the optimal waypoints of UAVs.

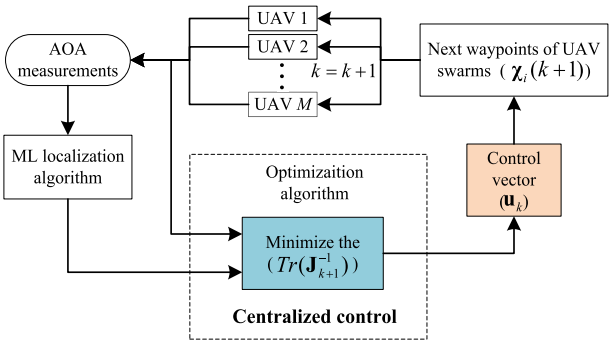

FIGURE 5. The flow chart of CRTO method.

Fig. 4 shows the target located by two UAVs, the objective function can be written as

$$\arg\min f\left(\chi_i(k+1), \mathbf{u}(k+1)\right) = \mathrm{Tr}\left(\mathbf{J}_{k+1}^{-1}\left(r_i, \theta_i\right)\right) \quad (37)$$

with,

$$\chi_i(k+1) = \begin{bmatrix} x_i(k) \\ y_i(k) \end{bmatrix} + v_0 T \begin{bmatrix} \cos u_i(k) \\ \sin u_i(k) \end{bmatrix} \quad (38)$$

$$\text{s.t. } \|u_i(k+1) - u_i(k)\| \le u_{\max} \quad (39)$$

$$\left\|\chi_i(k+1) - \hat{\mathrm{x}}_t(k)\right\| \le R_h \quad (40)$$

$$\left\|\chi_i(k+1) - \hat{\mathrm{x}}_t(k)\right\| \ge R_l \quad (41)$$

$$\left\|x_i(k+1) - \chi_j(k+1)\right\| \le c_h \quad (42)$$

$$\left\|\chi_i(k+1) - \chi_j(k+1)\right\| \ge c_l \quad (43)$$

Eq. (38) represents the state updating equation of the i-th UAV and Eq. (39) is the maximum optional heading angles boundary constraint. Eq. (40-41) indicates that there is a minimum and maximum distance constraints between UAV and target. Eq. (42) indicates the anti-collision constraint between any two UAVs. Eq. (43) is the maximum communication between UAVs.

To solve the above optimization, CRTO method needs to combine both real-time AOA measurements and state information of each UAV to the central processer. Fig. 5 shows the flow chart of CRTO method. The location of the target is estimated according to localization algorithms, i.e., maximum likelihood (ML) estimator [4], pseudo-linear estimator [2], etc. The target function shown in Eq. (36) is used for large-scale combined optimization. Variable space is solved by intelligent optimization algorithms such as heuristic or hyper-heuristic algorithm, and then the optimal heading of UAV swarms combination is obtained by searching for the optimal heading. Finally, the optimal heading instructions of each moment are continuously distributed to other UAVs through robust airborne data link [28]. According to the engineering experience, the time delay of more than 2 seconds caused by the real-time optimization calculation of the combined heading angles and the distribution of heading instructions for each UAV is easy to reduce the accuracy and tracking stability.

V. DISTRIBUTED COLLABORATIVE AUTONOMOUS GENERATION (DCAG) METHOD

A. THE FRAMEWORK OF DCAG

Aiming at the problem of long time delay caused by CRTO method, the DCAG method proposed in this paper applied the value of CRLB, which directly reflects the influence of configuration on localization accuracy. The configuration data of large samples of UAV swarms and target are generated by off-line simulation on the ground, and the optimal heading combination of UAV under each configuration is obtained off-line by theoretical analysis in Sec. III. Then, the labeled data set for each UAV is constructed for deep neural network. After the realization of off-line training and testing phases, this neural network loaded in each UAV can be applied online, as shown in Fig. 6.

The flow chart of DCAG method in online phase is shown in Fig. 7, compared with CRTO method, all UAVs only need to share their location information and measurement at each time step. When the target state is estimated, the optimal heading angles can be generated quickly and autonomously based on deep neural network, thus avoiding the long time delay caused by on-line real-time optimization of NP-hard problem.

At the same time, because of the implicit law of optimal heading angles combination are learned by off-line neural networks, on-line generations are naturally the optimal solutions, thus avoiding the communication delay caused by the central processer in CRTO method.

B. DEEP NEURAL NETWORK CONSTRUCTION

In order to realize on-line optimal heading angles generation of UAV swarms to reduce the localization error, it is necessary to take the current distance and angle of all UAVs to the target as the input of each UAV neural network. Under the unknown target location, the target passive location estimation is approximated to the true target position. The output of neural network is designed to optimize the heading angles of the UAV at the next moment. The neural network structure

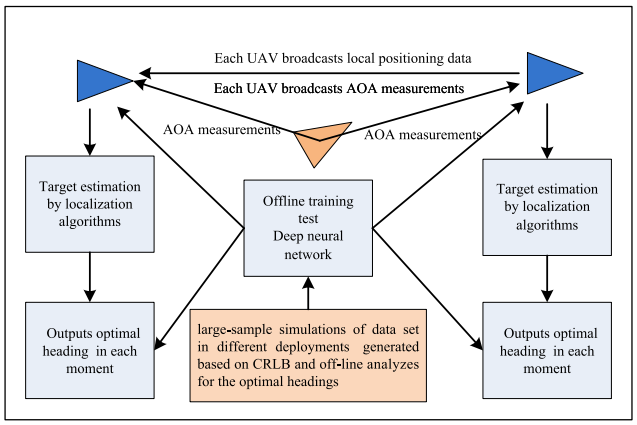

FIGURE 6. The framework of DCAG method.

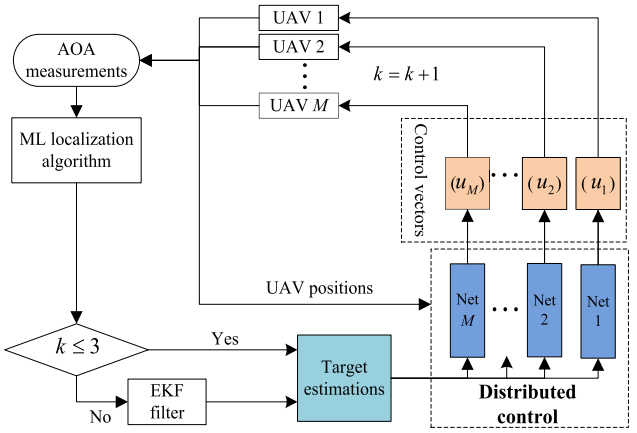

FIGURE 7. The flow chart of DCAG method in online phase.

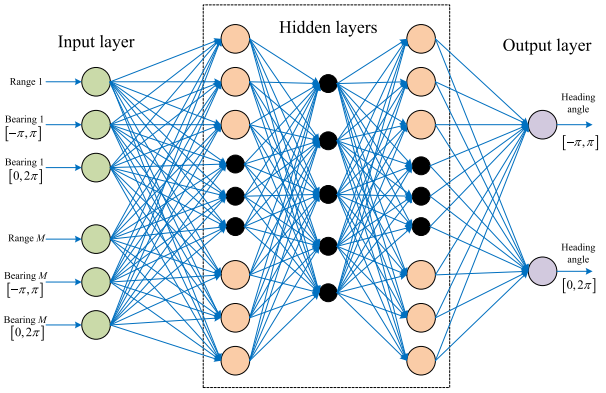

FIGURE 8. The neural network structure.

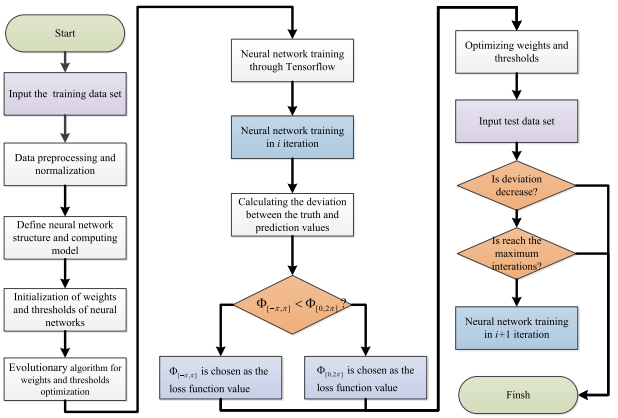

FIGURE 9. Off-line training and testing flow chart based on Tensorflow network.

adopts multiple hidden layers and full connection structure. When given M UAVs, an alternative choice for hidden layers can be set to M and the number of nodes per hidden layer can be set to $2M$.

Fig. 8 shows the input-output and structure of neural network for M UAVs. Here, we notice that when the intersection angle between optimal heading and target is close to π rad, the prediction heading is close to $-\pi$ rad in the process of neural network training. Although the prediction heading and optimal heading are in the same directions, the neural network will be mistaken for a large deviation when the single coordinate axis of $[\pi, -\pi]$ is used, which will affect the learning efficiency of neural network. Therefore, in this paper, two coordinate representations of $[-\pi, \pi]$ and $[0, 2\pi]$ are applied for both input and output angles of the neural network.

C. OFF-LINE NETWORK TRAINING TEST

After the data set and label set are constructed according to the input and output of the neural network for UAV heading decision-making, the off-line training and learning of the network is carried out by using Tensorflow platform [29]. Fig. 9 shows the offline training and testing flow chart based on Tensorflow platform. Three aspects should be noticed in the training process: Firstly, the predicted heading angles are calculated in two coordinate axes. By subtracting from the optimal heading angles, the minimum deviation is chosen as the loss function value; Secondly, evolutionary algorithm [30] are applied to optimize the weights and thresholds of the network; Thirdly, in order to prevent over-fitting of the network, the network is tested by the training data set to judge whether the loss function value is continuously reduced and this can be one of the termination conditions in the training phase.

VI. SIMULATION ANALYSIS

A. SIMULATION EXAMPLE DESCRIPTION

The validity of the proposed DCAG method is verified by a simulation example of two UAVs conducting AOA localization, and the parameter settings are as follows: 1) the path-loss exponent of AOA localization is $a = 0.01$; 2) UAV completes 50 direction finding signal sampling times per second; 3) the maximum and minimum distances between the target and UAV are $R_h = 20$km, $R_1 = 1$km, respectively; 4) The minimum distance between the two aircraft is $c_l = 200$m; 5) The data set of the optimal decision-making neural network for

TABLE 1. Example of dual machine cooperative passive location data set.

Training data set for UAV 1					Training data set for UAV 2				
r_1	$\phi_{1,[-\pi,\pi]}$	$\phi_{1,[0,2\pi]}$	$\Phi_{1,[-\pi,\pi]}$	$\Phi_{2,[0,2\pi]}$	r_2	$\phi_{2,[-\pi,\pi]}$	$\phi_{2,[0,2\pi]}$	$\Phi_{[-\pi,\pi]}$	$\Phi_{2,[0,2\pi]}$
4059	1.53	0.96	0.01	0.43	2861	-0.05	4.99	-2.43	1.79
11056	-1.13	3.29	0.81	0.34	2769	0.16	5.01	2.8	0.51
12416	2.27	2.79	0.02	2.04	11281	0.46	5.64	-2.34	1.69
14099	-2.08	5.16	0.23	4.41	5051	2.3	1.82	2.19	0.77
10567	0.32	3.56	-2.9	5.54	2492	-1.84	3.19	-1.11	0.58
2912	-2.72	5.09	-2.73	5.41	11609	1.97	0.6	1.68	3.69
6076	-2.18	5.68	-0.89	5.48	2977	0.13	3.71	1.74	0.79
2121	1.88	3.63	-1.09	1.18	5852	-0.06	4.57	2.03	1.75
7488	-0.06	0.64	2.23	6.08	3737	1.19	2.37	-3.14	5.21
9566	-0.12	0.94	-1.54	1.71	3633	-3.07	2	-2.42	0.44
.....	.....	.....	.....	.....	.....	.....	.....	.....	.....

off-line training of AOA localization of each UAV is shown in Tab. 1. $\phi_{[-\pi,\pi]}$ and $\phi_{[0,2\pi]}$ are the AOA measurements, which are defined such that $[-\pi, \pi]$ and $[0, 2\pi]$, respectively. $\Phi_{[-\pi,\pi]}$ and $\Phi_{[0,2\pi]}$ are the optimal heading angles in two coordinates.

B. VALIDATION OF DCAG METHOD

According to the optimal navigation data set given in Table 1, the depth neural network of UAV 1 and UAV 2 is trained off-line, and the hidden layer of the network is set to be 4 layers with 12 nodes per layer. In the off-line training phase of the network, the prediction mean deviation of each generation on the training data set and the test data set is observed and recorded simultaneously. As shown in Fig. 10, it can be seen that the depth neural network of UAV1 and UAV2 descends from the initial average 90 degree prediction deviation to average 5 degree deviation after 100 generations of training, and the prediction deviation on the test data sets also continues to decline, which indicate that the trained neural network has not been fitted and has generalization ability.

The initial neural network, training 100 generation, training 1000 generation and training 10000 generation neural network are loaded into the corresponding UAV, and put into the simulation environment of passive location of mobile target by two UAVs to carry out the actual operation. The effect of on-line operation under different algebras of neural network training is observed.

As shown in Fig. 11, the neural network generated by the initial randomization does not have any ability to optimize the heading angles without learning; After 100 iterations of training, each UAV equipped with neural network begins to learn to adjust and optimize the heading angles in real time according to the estimated position of the target and the position of the other UAV; After 1000 iterations of training, the UAVs follows with the target. After 10000 iterations of training, the average deviation between the predicted and the optimal heading angles have also reached below 1 degree. The accuracy of target positioning is continuously improved

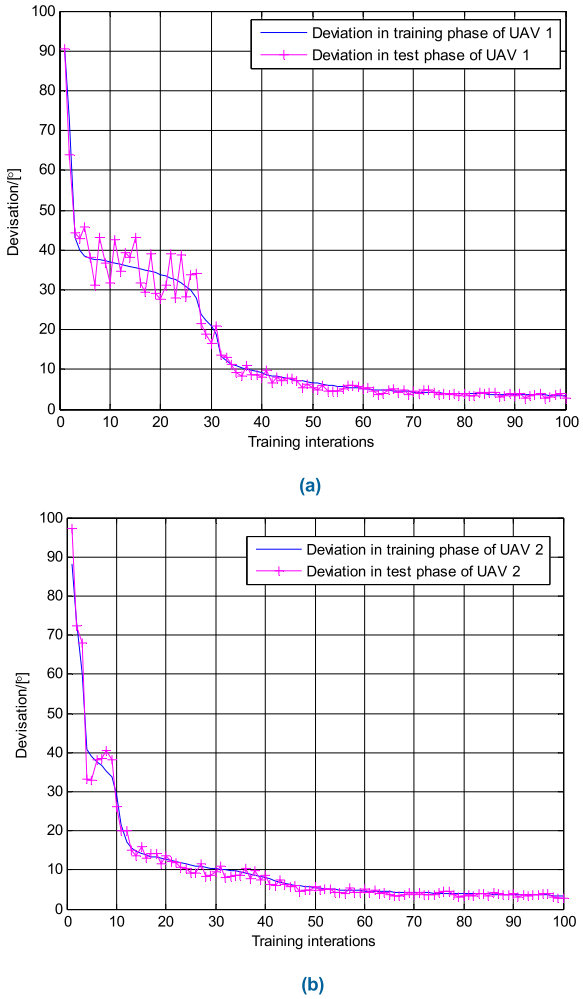

FIGURE 10. The evolution of the deviation in training and testing phases of different UAVs. (a) Evolution of deviation in training and test phases of UAV1. (b) Evolution of deviation in training and test phases of UAV2.

and the stable tracking is achieved. Thus, the neural network construction is accomplished.

C. THE PERFORMANCE OF DCAG METHOD

In this section we verify the analysis of the optimal AOA localization deployments shown in Sec. III. Two and three UAVs are applied to localize the target, respectively. When the target is stationary, the target motion model is given by $F_k = [1, 0; 0, 1]$. The true target location is $\mathbf{x}_t = [0, 0]^T$, the initial states of UAVs are $\mathbf{x}_1(1) = [-9600, -5000]^T$, $\mathbf{x}_2(1) = [-10000, -5000]^T$, $\mathbf{x}_3(1) = [-10000, -5400]^T$. The initial heading angles for UAVs are all equal to $\pi/2$ (y axis) with constant velocity $v_0 = 100m/s$and the heading angle constraint is $u_{\max} = 15°$.

From Figs. 12(a) and (b), it is obvious that each UAV tries to fly away from each other and tries to obtain a bigger angular separation φ_{12} to meet the angle criterion. At the same time, each UAV does not obtain sufficient target information because of the poor initial deployment. After about the 15th time step, the localization error decreases sharply with the changes of φ_{12}. After the 80 time steps, φ_{12} is

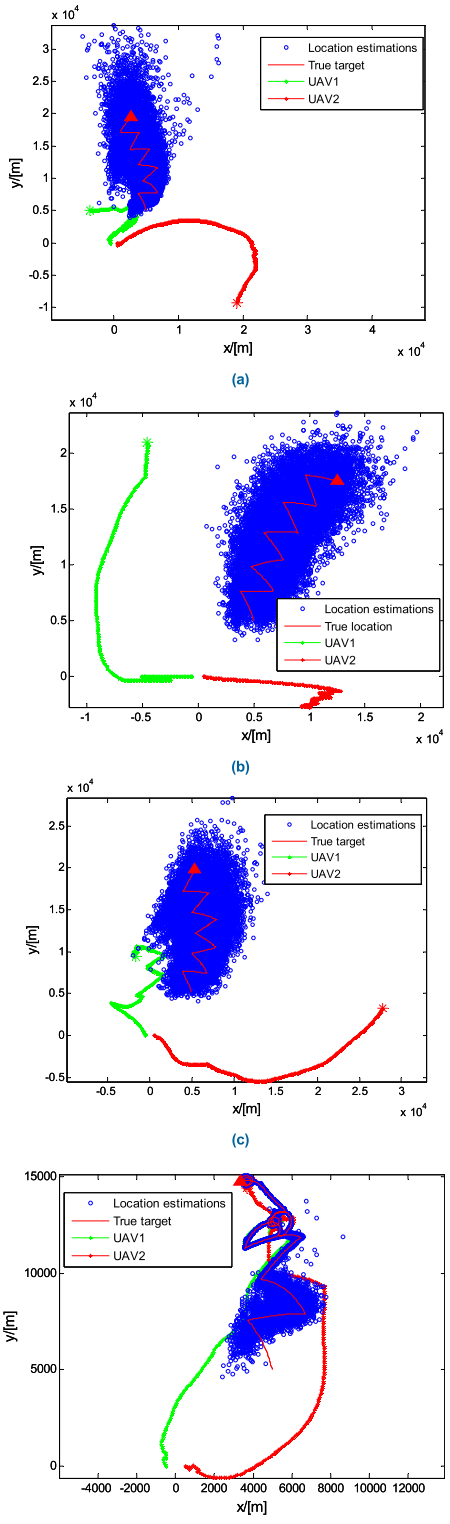

FIGURE 11. The performance of deep neural network online using with different iterations. (a) Initial randomization. (b) 100 iterations. (c) 1000 iterations. (d) 10000 iterations.

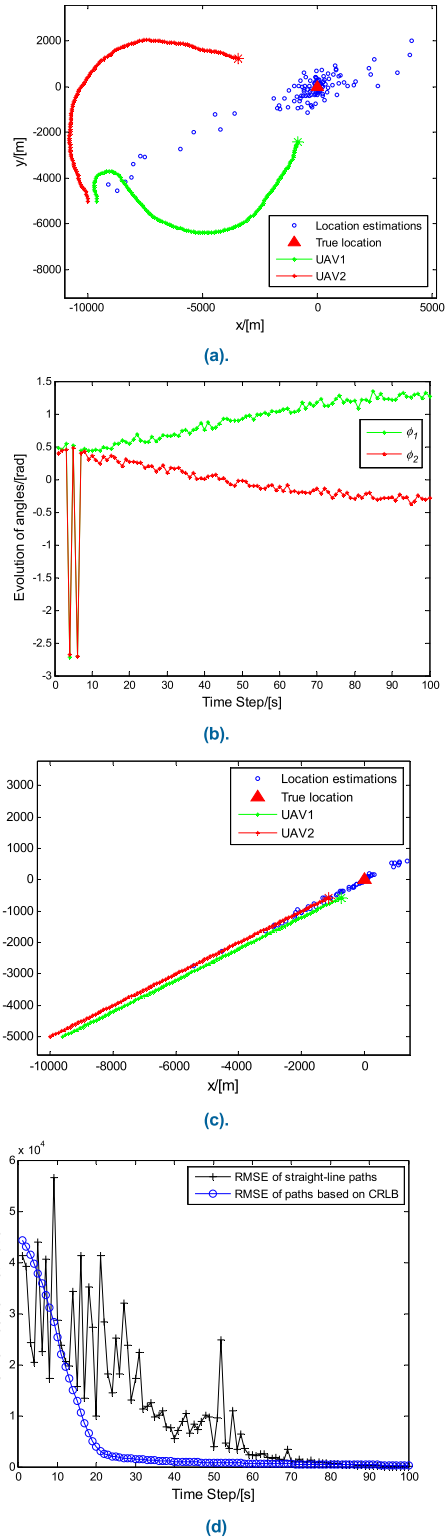

FIGURE 12. The performance of DCAG method with two UAVs. (a) Generated paths based on DCAG method for two UAVs. (b) Evolution of angles. (c) Straight-line paths. (d) Evolution of RMSE of paths based on CRLB and straight-line paths.

approximately equal to $\pi/2$. Then the UAVs begin to fly toward to target to get lower CRLB, and localization error almost converges to zero.

In addition, AOA localization without the trajectory optimization is also considered. Fig. 12(c) shows the straight-line paths of UAV swarms, whereby each UAV flies directly

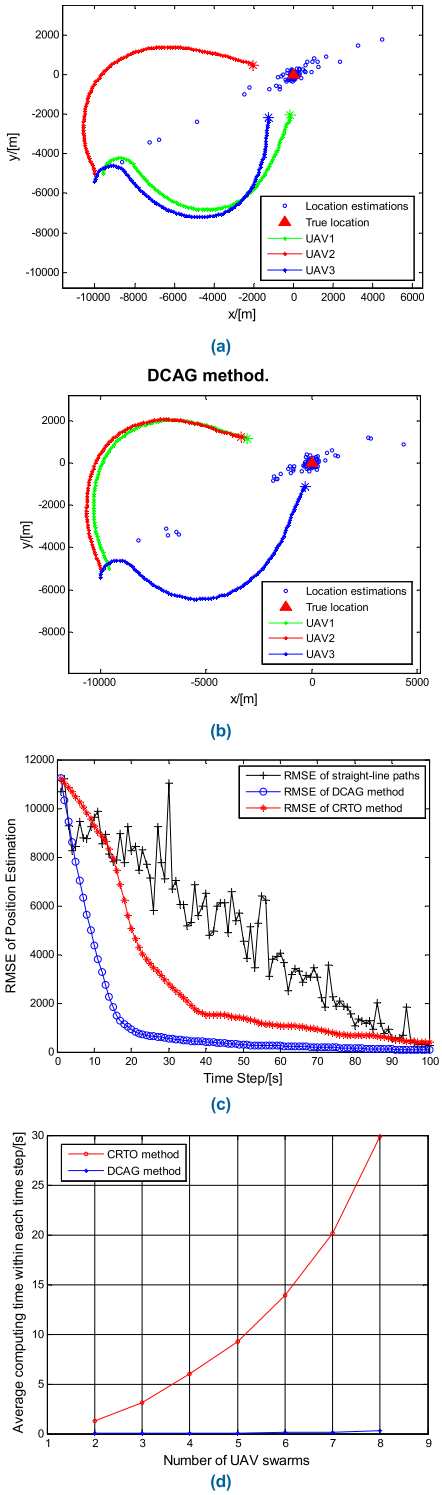

FIGURE 13. The performance of DCAG method. (a) The first classical generated paths for three UAVs based on DCAG method. (b) The second classical generated paths for three UAVs based on the CRLB. (c) Performance comparison of generated paths based on DCAG method, CRTO method and straight-line paths. (d) Performance comparison of average computing time based on DCAG and CRTO method.

towards the estimated target position. Fig. 12(d) shows the root mean squared error (RMSE) of paths based on CRLB compared with straight-line paths after 1000 times of

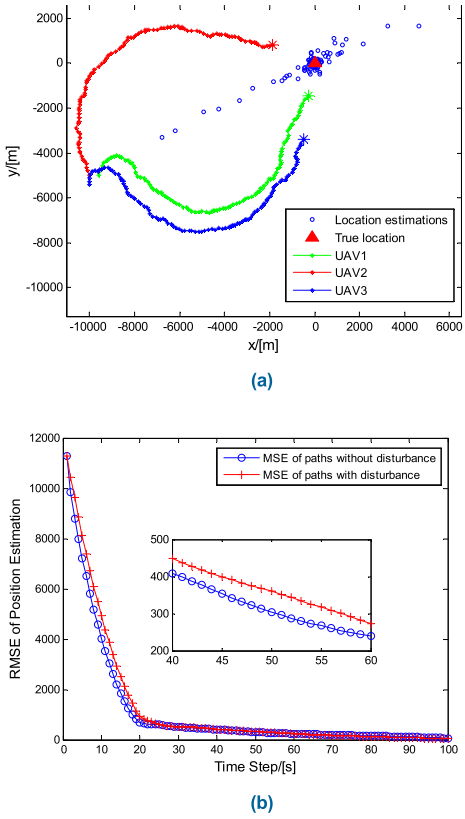

FIGURE 14. The performance of DCAG method in turbulence. (a) Generated paths based on DCAG for three UAVs with disturbance. (b) Evolution of RMSE of paths with disturbance and without disturbance based on DCAG.

Monte-Carlo simulation. Clearly it can be seen that angle criterion is able to reduce the location error stably. Meanwhile, the location error without path optimization is large and obviously uncertain.

The localization performances with three UAVs are included in the optimization problem. Two classical simulation results are shown in Figs. 13.

From Fig. 13(a) and Fig. 13(b), UAV swarms tend to expand the angular separations to have a better observation of the target. For the first classical generated paths, after about the 75th time step, the distances between each UAV and the target are almost equal, UAV3 begins to fly away from the UAV1, according to the angle criterion in the *Corollary*2. The optimal deployments can be acquired when $\varphi_{12} = \pi/3$ or $\varphi_{12} = 2\pi/3$. For the second classical generated paths, when one of the UAV (UAV3) flies much closer to the target compared with the other UAVs, i.e., the optimal deployment is $\varphi_{13} = \varphi_{23} = \pi/2$. Therefore, the analysis of optimal deployments and simulations help us to understand and improve the resultant UAV paths performance in the realistic case.

Fig. 13(c) shows the performance comparison of generated paths based on DCAG method, CRTO method and straight-line paths. The RMSE of UAV swarms in straight-line paths generally tends to decrease, which is mainly in

terms of the distance criterion. However, the localization accuracy is still unstable with poor deployments. DCAG method has lower RMSE than CRTO method and we can easily find that our proposed method has a much better source localization performance with the lower computation complexity.

In order to further illustrate the advantages of DCAG method, Fig. 13(d) shows the average computing time within each time step (Processor: Intel i7-6500U, 2.50GHz) of different numbers of UAV swarms compared with CRTO method. The average computing time of DCAG method ranges from 2.64×10^{-3} to 1.65×10^{-2} seconds when the number of receivers ranges from 2 to 8. Whereas, the average computing time of CRTO method ranges from 1.28 to 29.12 seconds in the same condition. This is mainly because of time consuming of optimization algorithm in each time step. With the increasing number of UAV swarms, the advantages of DCAG method will be more prominent.

D. TURBULENCE EFFECTS IN DCAG METHOD

In the real application, UAV swarm may be disturbed by random wind gusts. The effect of wind can be modeled by the Dryden model [31]. Dryden model is one of the most useful models for atmospheric turbulence. To define it, the turbulence is modeled as a random velocity process added by the UAV swarms velocity vector in body-fixed coordinate system.

Let $\psi_i(k)$ be the wind direction, K be a scale factor representing the wind gust strength, the disturbed UAV locations is given by

$$\mathbf{q}_i(k) = (\bar{v} + \kappa v_i(k)) \begin{bmatrix} \cos \psi_i(k) \\ \sin \psi_i(k) \end{bmatrix} \tag{44}$$

where $\bar{v}$ is the mean wind noise, $v_i(k)$, i=1, $\cdots$, M is a correlated Gaussian noise sequence. The actual location of disturbed UAV at time step k is $\mathbf{x}_i(k+1)+\mathbf{q}_i(k)$, where $\mathbf{x}_i(k+1)$ is the calculated optimal waypoint.

The trajectories of UAV swarms with disturbance are presented in Fig. 14(a). The wind parameters are $\psi_i(k) = \pi/4$, $\bar{v} = 20m/s$ and $\kappa = 10$. It can be seen that the UAV swarms cannot reach the theoretical waypoints (shown in Figs. 13(a) and (b)).

Fig. 14 (b) shows the RMSE performance of the UAV with disturbance. It is clear that the error with disturbance is slightly higher than that of receiver without disturbance. However, the planning algorithm is still efficient to achieve a better performance. No accumulation of errors in DCAG method is added in each time step, since the path planning optimization is done with a set of control vectors.

VII. CONCLUSION

In this paper, the analytic solutions of optimal receiver-target deployment in AOA localization were investigated when the noise variance was distance-dependent. The both angle and distance criterions were acquired, which can provide the understanding of the paths of in AOA localization. UAV path planning algorithm was extended under motion and communication constraints. The DCAG method base on deep neural network was proposed. Compared with the traditional CRTO method, the DCAG method has three advantages: Firstly, it transforms the online real-time optimization NP-Hard problem into the off-line machine learning problem, thus reducing the computation delay; Secondly, it transforms the central UAV control mechanism into the continuously distributed heading angles for each UAV. The self-synchronization mechanism of distributed autonomous cooperative optimal control vector reduces the delay caused by communication distribution. Thirdly, the distributed UAV passive location network formed by DCAG is a decentralized structure, which increases the survivability and robustness of the UAV network under actual combat conditions. The simulation analysis showed that UAV swarms complied with angle and distance criteria when searching for optimized path and it was also affected by its own constraints. Analysis of optimal deployments was verified by simulation examples and a good agreement between the theory and simulations was achieved.

Future extensions for this paper are to consider the instantaneous motion constraints, three-dimensional terrain environment, complex electromagnetic environment and multi-target scenario in real UAV swarms application.

ACKNOWLEDGMENT

The authors sincerely thank the anonymous reviewers for their valuable and constructive comments.

REFERENCES

[1] Y. Zou, H. Liu, W. Xie, and Q. Wan, "Semidefinite programming methods for alleviating sensor position error in TDOA localization," *IEEE Access*, vol. 5, pp. 23111–23120, 2017.

[2] H.-J. Shao, X.-P. Zhang, and Z. Wang, "Efficient closed-form algorithms for AOA based self-localization of sensor nodes using auxiliary variables," *IEEE Trans. Signal Process.*, vol. 62, no. 10, pp. 2580–2594, May 2014.

[3] A. N. Bishop and P. Jensfelt, "An optimality analysis of sensor-target geometries for signal strength based localization," in *Proc. ISSNIP*, Dec. 2009, pp. 127–132.

[4] M. Gavish and A. J. Weiss, "Performance analysis of bearing-only target location algorithms," *IEEE Trans. Aerosp. Electron. Syst.*, vol. 28, no. 3, pp. 817–828, Jul. 1992.

[5] S. C. Nardone, A. G. Lindgren, and K. F. Gong, "Fundamental properties and performance of conventional bearings-only target motion analysis," *IEEE Trans. Autom. Control*, vol. 29, no. 9, pp. 775–787, Sep. 1984.

[6] V. J. Aidala, "Kalman filter behavior in bearings-only tracking applications," *IEEE Trans. Aerosp. Electron. Syst.*, vol. AES-15, no. 1, pp. 29–39, Jan. 1979.

[7] K. Spingarn, "Passive position location estimation using the extended Kalman filter," *IEEE Trans. Aerosp. Electron. Syst.*, vol. AES-23, no. 4, pp. 558–567, Jul. 1987.

[8] A. N. Bishop, B. Fidan, B. D. O. Anderson, K. Dogancay, and P. N. Pathirana, "Optimality analysis of sensor-target geometries in passive localization: Part 1-Bearing-only localization," in *Proc. 3rd Int. Conf. Intell. Sensors, Sensor Netw. Inf.*, Melbourne, Qld., Australia, Dec. 2007, pp. 7–12.

[9] K. Doğançay and H. Hmam, "Optimal angular sensor separation for AOA localization," *Signal Process.*, vol. 88, pp. 1248–1260, May 2008.

[10] A. N. Bishop, B. Fidan, B. D. O. Anderson, K. Doğançay, and P. N. Pathirana, "Optimality analysis of sensor-target localization geometries," *Automatica*, vol. 46, no. 3, pp. 479–492, 2010.

[11] S. Xu and K. Doğançay, "Optimal sensor placement for 3-D angle-of-arrival target localization," *IEEE Trans. Aerosp. Electron. Syst.*, vol. 53, no. 3, pp. 1196–1211, Jun. 2017.
[12] P. Sarunic and R. Evans, "Hierarchical model predictive control of UAVs performing multitarget-multisensor tracking," *IEEE Trans. Aerosp. Electron. Syst.*, vol. 50, no. 3, pp. 2253–2268, Jul. 2014.
[13] K. Doğançay, "UAV path planning for passive emitter localization," *IEEE Trans. Aerosp. Electron. Syst.*, vol. 48, no. 2, pp. 1150–1166, Apr. 2012.
[14] T. Dierks and S. Jagannathan, "Output feedback control of a quadrotor UAV using neural networks," *IEEE Trans. Neural Netw.*, vol. 21, no. 1, pp. 50–66, Jan. 2010.
[15] C. Yang, C. Chen, W. He, R. Cui, and Z. Li, "Robot learning system based on adaptive neural control and dynamic movement primitives," *IEEE Trans. Neural Netw. Learn. Syst.*, vol. 30, no. 3, pp. 777–787, Mar. 2019.
[16] R. Lungu and M. Lungu, "Adaptive flight control law based on neural networks and dynamic inversion for micro-aerial vehicles," *Neurocomputing*, vol. 199, pp. 40–49, Jul. 2016.
[17] C. J. Kim, and D. Chwa, "Obstacle avoidance method for wheeled mobile robots using interval type-2 fuzzy neural network," *IEEE Trans. Fuzzy Syst.*, vol. 23, no. 3, pp. 677–687, Jun. 2015.
[18] S. X. Yang, A. Zhu, G. Yuan, and M. Q.-H. Meng, "A bioinspired neurodynamics-based approach to tracking control of mobile robots," *IEEE Trans. Ind. Electron.*, vol. 59, no. 8, pp. 3211–3320, Aug. 2012.
[19] D. Maravall, J. de Lope, and J. P. Fuentes, "Vision-based anticipatory controller for the autonomous navigation of an UAV using artificial neural networks," *Neurocomputing*, vol. 151, pp. 101–107, Mar. 2015.
[20] R. Kaune, J. Horst, and W. Koch, "Accuracy analysis for TDOA localization in sensor networks," in *Proc. 14th Int. Conf. Inf. Fusion*, Chicago, IL, USA, Jul. 2011, pp. 1647–1654.
[21] D. Ucinski, *Optimal Measurement Methods for Distributed Parameter System Identification*. Boca Raton, FL, USA: CRC Press, 2004.
[22] J. J. Benedetto and M. Fickus, "Finite normalized tight frames," *Adv. Comput. Math.*, vol. 18, no. 2, pp. 357–385, 2003.
[23] J. Kovacevic and A. Chebira, "Life beyond bases: The advent of frames (part I)," *IEEE Signal Process. Mag.*, vol. 24, no. 4, pp. 86–104, Jul. 2007.
[24] P. G. Casazza, M. Fickus, J. Kovacevic, M. T. Leon, and J. C. Tremain, *A Physical Interpretation of Tight Frames: Harmonic Analysis and Applications*. Boston, MA, USA: Birkhäuser, 2006.
[25] S. Zhao, B. M. Chen, and T. H. Lee, "Optimal placement of bearing-only sensors for target localization," in *Proc. Amer. Control Conf.*, Montreal, QC, Canada, Jun. 2012, pp. 5108–5113.
[26] W. Yan, X. Fang, and J. Li, "Formation optimization for AUV localization with range-dependent measurements noise," *IEEE Commun. Lett.*, vol. 18, no. 9, pp. 1579–1582, Sep. 2014.
[27] W. Meng, L. Xie, and W. Xiao, "Optimal TDOA sensor-pair placement with uncertainty in source location," *IEEE Trans. Veh. Technol.*, vol. 65, no. 11, pp. 9260–9271, Nov. 2016.
[28] S. Kemkemian, M. Nouvel-Fiani, and E. Chamouard, "Radar and electronic warfare cooperation: How to improve the system efficiency," *IEEE Aerosp. Electron. Syst. Mag.*, vol. 26, no. 8, pp. 32–38, Aug. 2011.
[29] J. Persano, S. M. Mikki, and Y. M. M. Antar, "Gradient population optimization: A Tensorflow-based heterogeneous non-von-Neumann paradigm for large-scale search," *IEEE Access*, vol. 6, pp. 77097–77122, 2018.
[30] H. Wang and J. Shen, "An improved model combining evolutionary algorithm and neural networks for PV maximum power point tracking," *IEEE Access*, vol. 7, pp. 2823–2827, 2019.
[31] M. Barbary and P. Zong, "Optimisation for stealth target detection based on stratospheric balloon-borne netted radar system," *IET Radar, Sonar Navigat.*, vol. 9, no. 7, pp. 802–816, Feb. 2015.

WEIJIA WANG received the B.S. and M.S. degrees from Air Force Engineering University, in 2013 and 2015, respectively. He is currently pursuing the Ph.D. degree in electronic science and technology, Air Traffic Control and Navigation College, Air Force Engineering University, Xi'an. His research interests include cooperative control of UAV, and sensor networks for radar and electronic warfare applications.

PENG BAI was born in 1961. He received the bachelor's degree in radar engineering from the School of Aeronautics and Astronautics Engineer, Air Force Engineering University, in 1983, and the master's degree in information and communication engineering from Northwestern Polytechnical University, in 1989. He is currently a Professor with the School of Equipment Development and Application Research Center, Air Force Engineering University. He has published more than 120 journal papers as the major author; among them, 30 articles were retrieved by SCI and 37 by EI. He is the Chief Expert and the main person responsible for a number of national key scientific research projects. His current research interests include advanced electronic science and technology in the future, and science and technology of network information system in the future. He received the National Science and Technology Progress Award for several times. He was commended by the President of China.

YU ZHOU was born in 1983. He received the M.S. degree from Air Force Engineering University and the Ph.D. degree from the National University of Defense Technology. He is currently a Lecturer with the Equipment Management & UAV Engineering College, Air Force Engineering University. His research interests include autonomous cognitive decision-making for UAV, deep reinforcement learning, and autonomy test and evaluation.

XIAOLONG LIANG was born in 1981. He received the master's degree in operational research and cybernetics and the Ph.D. degree in armament science and technology from Air Force Engineering University, where he is currently a Professor with the Air Traffic Control and Navigation College. He is a major of several national scientific research projects. He has published more than 50 journal papers and finished more than 20 projects. His research interests include aircraft swarm technology, airspace management intelligence, and intelligent aviation systems.

YUBING WANG was born in 1994. She received the M.S. degree from the Aeronautics and Astronautics Engineering College, Air Force Engineering University, Xi'an, in 2017. She is currently pursuing the Ph.D. degree with the Air Traffic Control and Navigation College, Air Force Engineering University. Her research interests include cooperative control of UAV swarms, wireless sensor networks, and intelligence optimization algorithm.